KFKI-1981-27

F. PÁSZTI
J. TAR
E. KÓTAI
A. MANUABA
T. LOHNER
G. MEZEY
L. PÓCS

PRELIMINARY RESULTS OF THE INVESTIGATION OF PLASMA CONTAMINATION IN MT-1 TOKAMAK ON PROBES BY RBS AND CHANNELING

Hungarian Academy of Sciences

CENTRAL RESEARCH INSTITUTE FOR PHYSICS

BUDAPEST

2017

KFKI-1981-27

PRELIMINARY RESULTS OF THE INVESTIGATION OF PLASMA CONTAMINATION IN MT-1 TOKAMAK ON PROBES BY RBS AND CHANNELING

F. Pászti, J. Tar, E. Kótai, A. Manuaba, T. Lohner,
G. Mezey, L. Pócs

Central Research Institute for Physics
H-1525 Budapest 114, P.O.B. 49, Hungary

HU ISSN 0368 5330
ISBN 963 371 804 X

ABSTRACT

Single-crystal silicon probes were placed near to the liner into the MT-l tokamak and impurities were collected under 203 and 751 plasma discharges. The radial distribution of the impurities were measured by RBS and channeling methods. Disordered layers were found both on electron and ion side.

АННОТАЦИЯ

Монокристаллические пленки кремния были положены коллектором в токамак МТ-1 при разряде 203 и 751 близко к камере. Распределение примесей по расстоянию от стенки камеры было измерено с помощью обратного рассеяния ионов и при использовании метода каналирования. Поврежденный слой находится на стороне ионов и электронов.

KIVONAT

Egykristályos szilicium minták gyüjtötték az MT-l-beli szennyezőket közel a liner-hez 203, illetve 751 kisülés alatt. Szennyezők sugárirányu eloszlását RBS és csatornahatás módszerekkel térképezték fel. Mind az ion, mind az elektron oldalon roncsolt rétegek találhatóak.

1. Introduction

Impurities originating from the interaction of plasma with the first wall of CTR devices are a troublesome factor causing energy loss from the plasma and leading to reduction in plasma temperature.

Several methods have been worked out partly to investigate the contamination of plasma, partly to study the various mechanism of the origin of these foreign atoms. The first kind of measurements are mainly based on the analysis of collector probes placed in tokamaks. Previous works were carried out using Rutherford backscattering or AES or SIMS [1,2,3,4,5,6].

The RBS method is a straightforward and non-destructive technique to measure the number of impurity atoms on the surface of solid materials.

The sensitivity of RBS in standard configuration /2 MeV $^4He^+$, $\Theta_s = 165^o$/ for light elements is in the range between 10^{15}-10^{16} atoms/cm^2 and for heavier elements it goes down to about 10^{12} atoms/cm^2.

Using special tricks: optimalization of the type of projectile ions, bombarding energy, scattering geometry etc. this values can be improved. For example, with heavier ions such as 2 MeV $^{14}N^+$ ions, 10^{-5} monolayer heavy impurity can be detected on the very surface. So in this respect the RBS is matching with SIMS which is generally regarded the most sensitive analysing method.

This paper deals with the first experimental study of impurities by RBS on collector probes placed in the MT-1 tokamak of Central Research Institute for Physics, Budapest.

2. Experimental

The detailed description of MT-1 tokamak will be published elsewhere. Here only the basic parameters of operation are quoted /Table 1./.

As collector probes single-crystal silicon samples were used /Fig. 1./ in two set of experiments. In both cases the probes were paralell with the minor radius and their polished surface were normal to the ion or the electron drift. In either experiment the long range impurity deposition was investigated. As the sample size was 10 x 15 mm, it allowed to measure the radial distribution of foreign species.

At the first configuration /Samples A/ the edge of probes were inside the limiter /d=1 mm/, the impurity accumulation was obtained as a result of 203 discharges. In the second case /samples B, d=-1 mm/ the effect of 751 discharges was accumulated.

After removing the probes they were subjected to Rutherford backscattering and channeling investigations with a standard RBS equipment in a vacuum of $2-5x10^{-7}$ torr.

Seeking the optimal experimental condition for different impurities the analysis was carried out in five different configurations /Table 2./. To plot the radial distribution of impurities both on the ion and the electron side the measurements were done along the probes with a lateral resolution of 1 mm.

For medium atomic numbers, where the mass separation of RBS is poor, computer deconvolution was applied, for example, on the Cr-Fe peak.

3. Results and discussion

The probes collected impurities in the range between 10^{12}-10^{17} atoms/cm^2 during the large number of discharges. Most of them exhibited radial distribution as it is shown on Fig. 2.,3.,4. for Fe Cr and Mo. The decrease of their quantities as moving away from the plasma was approximated as a straight line for samples A. After 751 discharges /samples B/ the radial distribution clearly showed a non-linear character.

Some impurities exhibited only weak radial dependence /for example Cu on Fig. 5./. It is reasonable to suppose that these atoms do not primarily originate from plasma interaction with the first wall but they comes from the vacuum versel e.g. during the backing out.

The Fig. 6. and 7. summarize the observations.

Elements lighter than silicon could only be investigated in channel direction where the silicon scattering yield decreases almost two order of magnitude. But we have to take into consideration that even virgin silicon samples are always covered by thin native oxide. Our experimental values were the same as in previous investigations [7]: 5×10^{15} O/cm^2 and 1.2×10^{16} Si/cm^2. Besides, during analysis carbon deposition is always detected. The rate of carbon deposition is specific to the corresponding vacuum system. In our goniometer this rate was as low as 0.05 C/$^4He^+$ using a special cold-trap system. The typical carbon deposition was 5×10^{15} cm^2, our rough oxygen, carbon and silicon data were corrected by substraction of the corresponding values.

Perhaps the most interesting results were obtained from channeling measurements because strongly disordered surface was found both on the electron and ion side at the nearest points to the plasma /Fig. 8. and Fig. 9./. On the figures aligned scattering yield normalized to the random yield is shown as the function of depth. The numbers at the curves mean the distance from the inner side of liner in mm units.
As the spectra were taken by glancing detection, the special scattering geometry provided 5 nm depth resolution.

The normalized yield functions are in correlation with the disorder density at a given depth, so with the degree of amorphousness in the surface region. The thin films spectra were converted into rectangular signals assuming the system resolution to be Gaussian [8].

The results of the deconvolution calculation together with the substraction of the amount of silicon originating from the native oxide are shown on Fig. 10. for samples B. It seems that on the ion side fully amorphous layers with thicknesses from 2 to 6 nm are present. This disorder is likely due to the highest energy part of ionic and/or neutral hydrogen atoms escaped from the plasma and are implanted into the probe but this speculation is far from being satisfactory.

On the electron side the situation is different. Thicker layers with lower degree of amorphousness can be detected. The deeper penetration, the lower disorder concentration, the lack of sharp interface suggest that this phenomenon is mainly caused by electron bombardment.

Finally we would like to point at the difficulties of the interpretation of the results. First of all the sticking coefficients of different impurities are unknown. The second problem follows from the long-time collection. One can not predict the effect of subsequent discharges on species which are already on the surface. We, however, believe our results together with other methods might give contribution to the description of impurity transport in tokamaks.

Table 1.

Some data about the MT-1 tokamak

Major radius	40 cm
Plasma radius /Mo limiter/	9 cm
The radius of liner	10 cm
H gas pressure before discharge	2-3x10^{-4} torr
Plasma current	25-30 kA
Pulse length	8.5 ms
Loop voltage	3-3.5 V
Toroidal magnetic field	1-1.2 T
Max. electron temperature	500 eV
Max. ion temperature	100 eV

Table 2.

Experimental conditions during analysis

	Energy Mev	Projectile	Scattering angle	Solid angle of detection msr	Type	Symbol on figs.
1.	2	$^{4}He^{+}$	165^{o}	0.7	RBS, channeling	○
2.	2	$^{4}He^{+}$	165^{o}	7	RBS, channeling	△
3.	2	$^{14}N^{+}$	165^{o}	0.7	RBS	×
4.	2	$^{14}N^{+}$	165^{o}	7	RBS	+
5.	2	$^{4}He^{+}$	97^{o}	0.3	RBS, channeling	

References

1. G. Dearnaley, G.M. McCracken, J.F. Turner and J. Vince, Nucl. Instr. Meth. 149 253 /1978/
2. G.M. McCracken, G. Dearnaley, S.J. Fielding, D.H.J. Goodall, J. Hugill, J.W.M. Paul, P.E. Stott, J.F. Turner and J. Vince, Proc. of 8th Europ. Conf. on Controlled Fusion and Plasma Physics, Prague, 1977, p. 40.
3. G.M. McCracken, G. Dearnaley, R.D. Gill, J. Hugill, J.W.M. Paul, B.A. Powell, P.E. Stott, J.F. Turner and J.E. Vince, J. Nucl. Mat. 76-77 431 /1978/
4. W.R. Wampler, S.T. Picraux, S.A. Cohen, H.F. Dylla, S.M. Rossnagel and G.M. McCracken, J.Nucl. Mat. 93-94 139 /1980/
5. V.M. Chicherov, D. Hildebrant, M. Laux, J. Lingertat, S.U. Lukianov, P. Pech, H.-D. Reiner, V.A. Stepanchikov and H. Wolf, J. Nucl. Mat. 93-94 133 /1980/
6. J.B. Roberts, R.A. Zuhr and S.P. Withrow, J. Nucl. Mat. 93-94 146 /1980/
7. W.K. Chu, E. Lugujjo, J.W. Mayer and T.W. Sigmon, Thin Solid Films, 19 329 /1973/
8. W.K. Chu, J.W. Mayer, M-A. Nicolet, Backscattering Spectrometry, Academic Press, 1978, p. 328

Figure captions

Fig. 1. Schematic configuration of silicon probes in MT-1

Fig. 2/a Radial distribution of iron on the ion side

Fig. 2/b Radial distribution of iron on the electron side

Fig. 3/a Radial distribution of Chromium on the ion side

Fig. 3/b Radial distribution of Chromium on the electron side

Fig. 4/a Radial distribution of Molybdenum on the ion side

Fig. 4/b Radial distribution of Molybdenum on the electron side

Fig. 5/a Radial distribution of Copper on the ion side

Fig. 5/b Radial distribution of Copper on the electron side

Fig. 6. Summarizing picture of the radial distribution of impurities after 203 plasma discharges

Fig. 7. Summarizing picture of the radial distribution of impurities after 751 plasma discharges

Fig. 8. Normalized disorder function on the ion side of sample B

Fig. 9. Normalized disorder function on the electron side of sample B

Fig. 10. The thickness of disorder and the degree of amorphousness after deconvolution on sample B

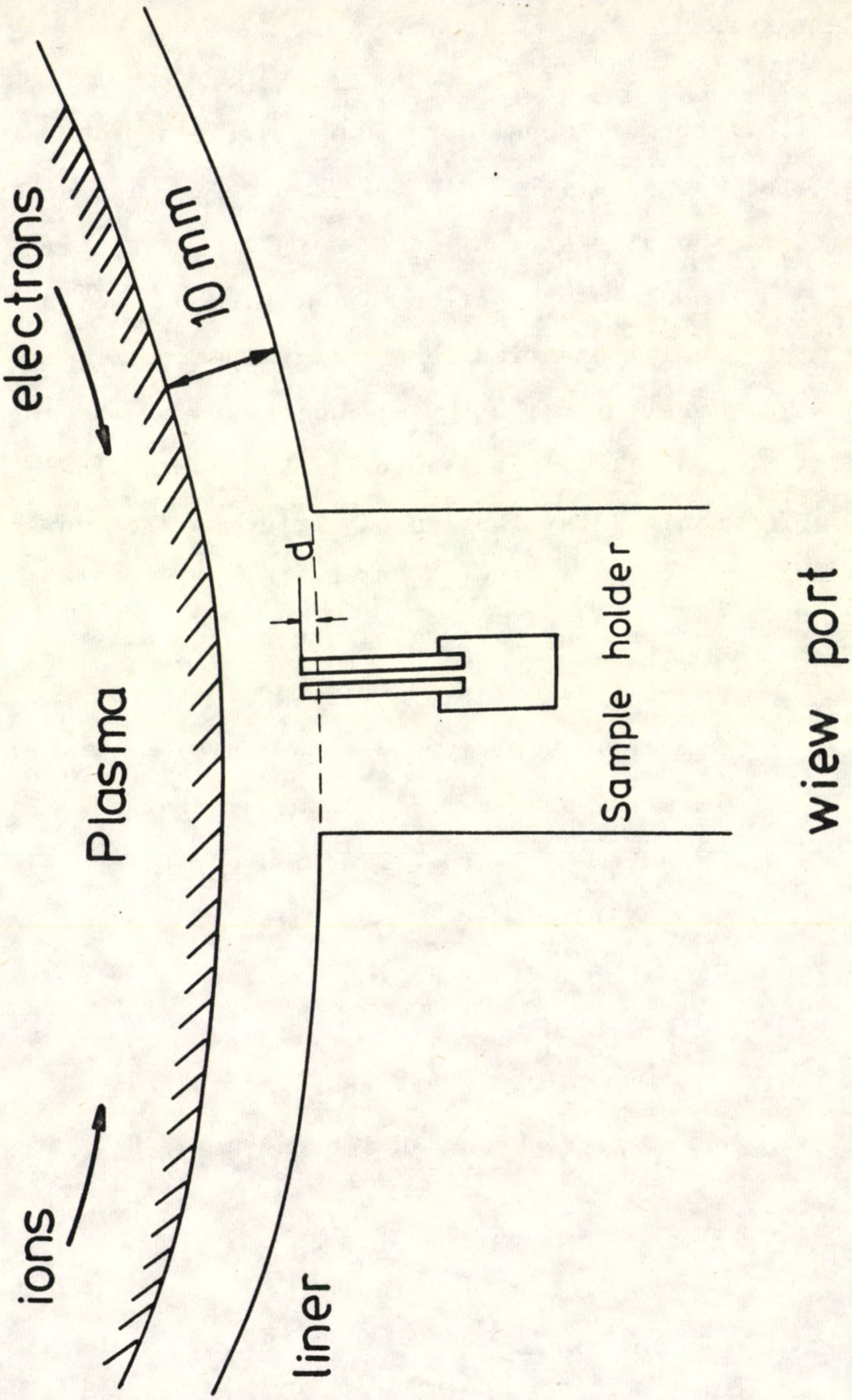

Fig.1.

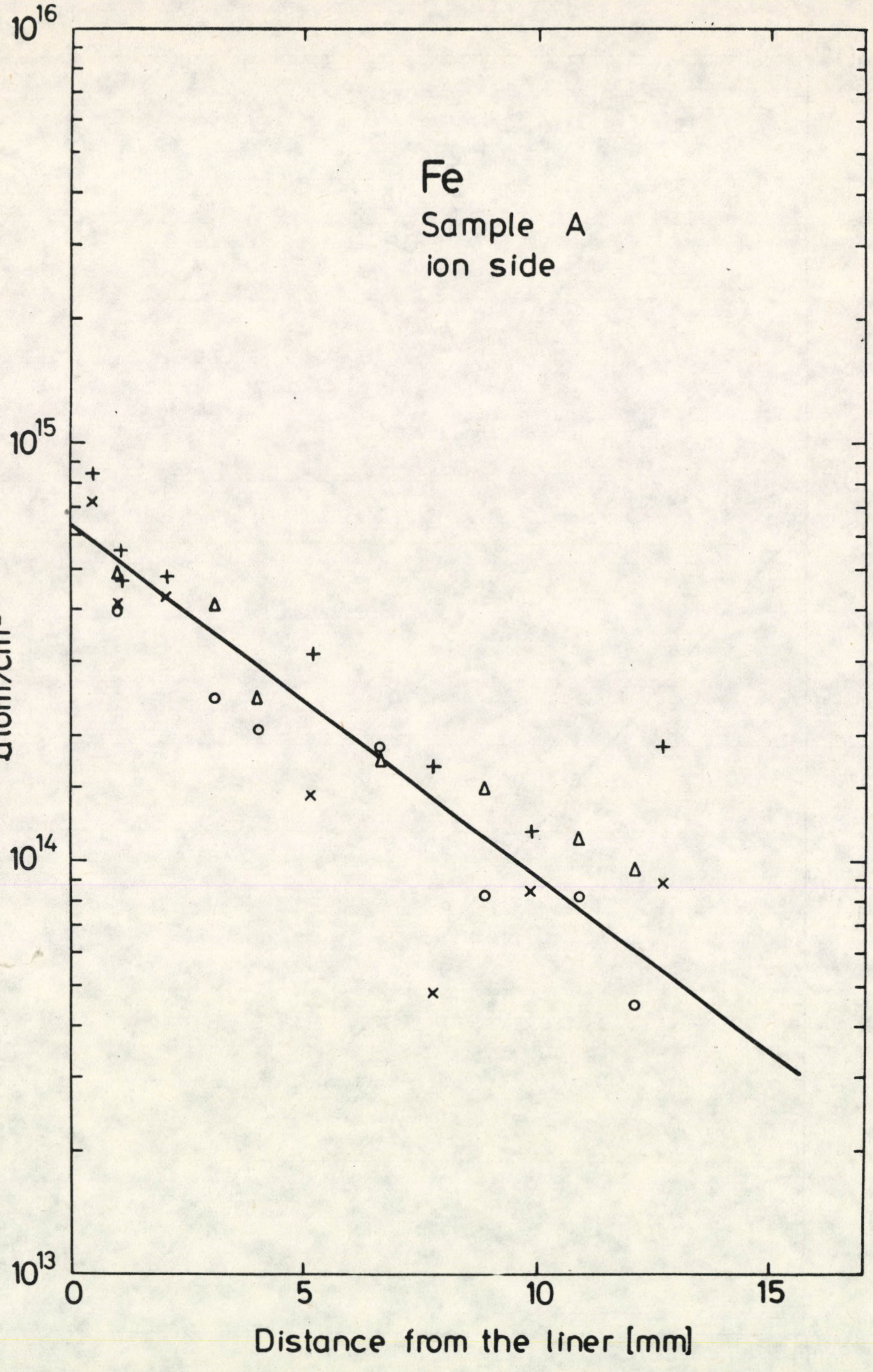
Fe
Sample A
ion side
10^{16}
10^{15}
10^{14}
10^{13}
atom/cm^2
0
5
10
15
Distance from the liner [mm]

Fig. 2a

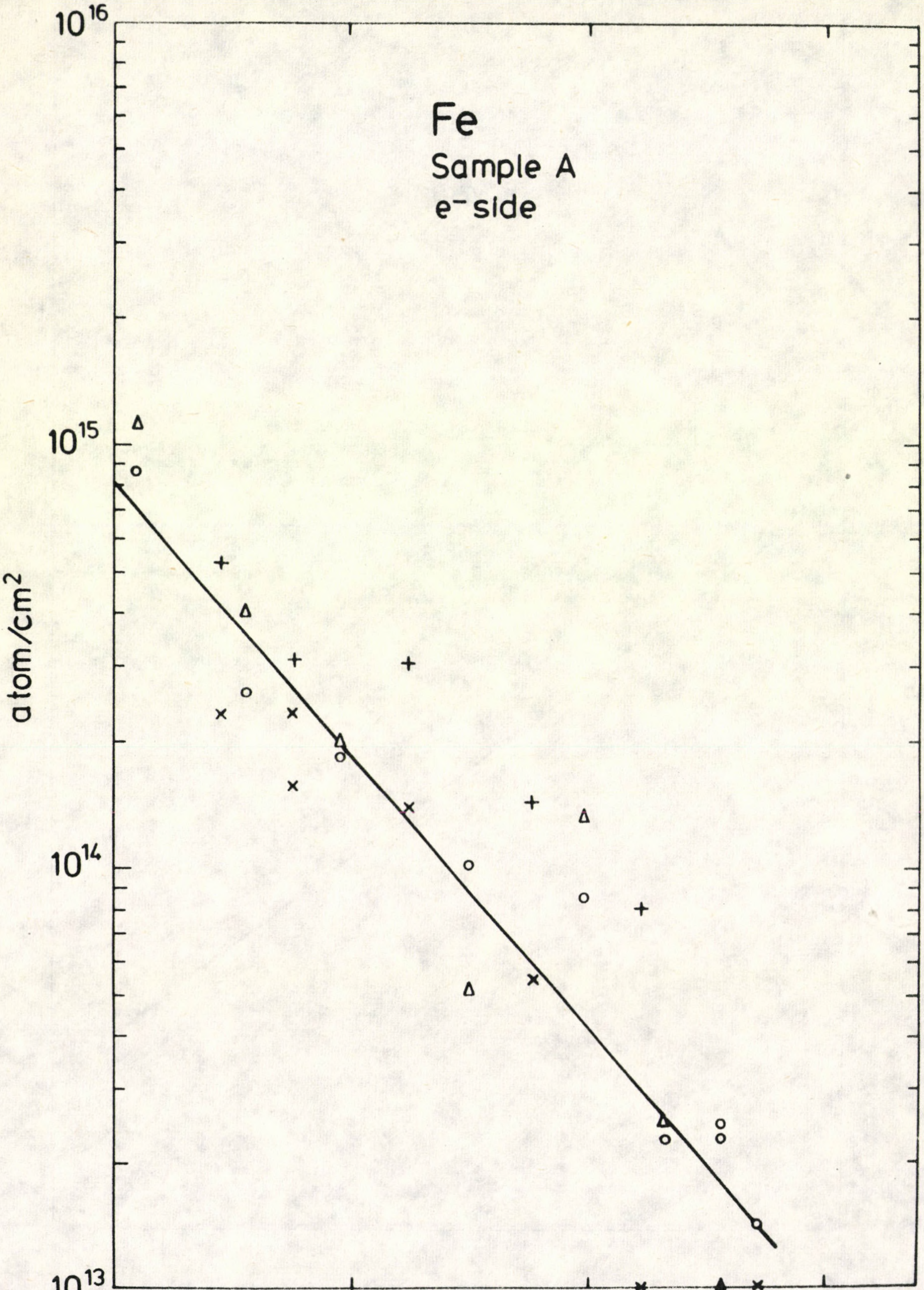
Fe
Sample A
e⁻side
atom/cm²
10^16
10^15
10^14
10^13
0
5
10
15
Distance from the liner [mm]

Fig. 2b

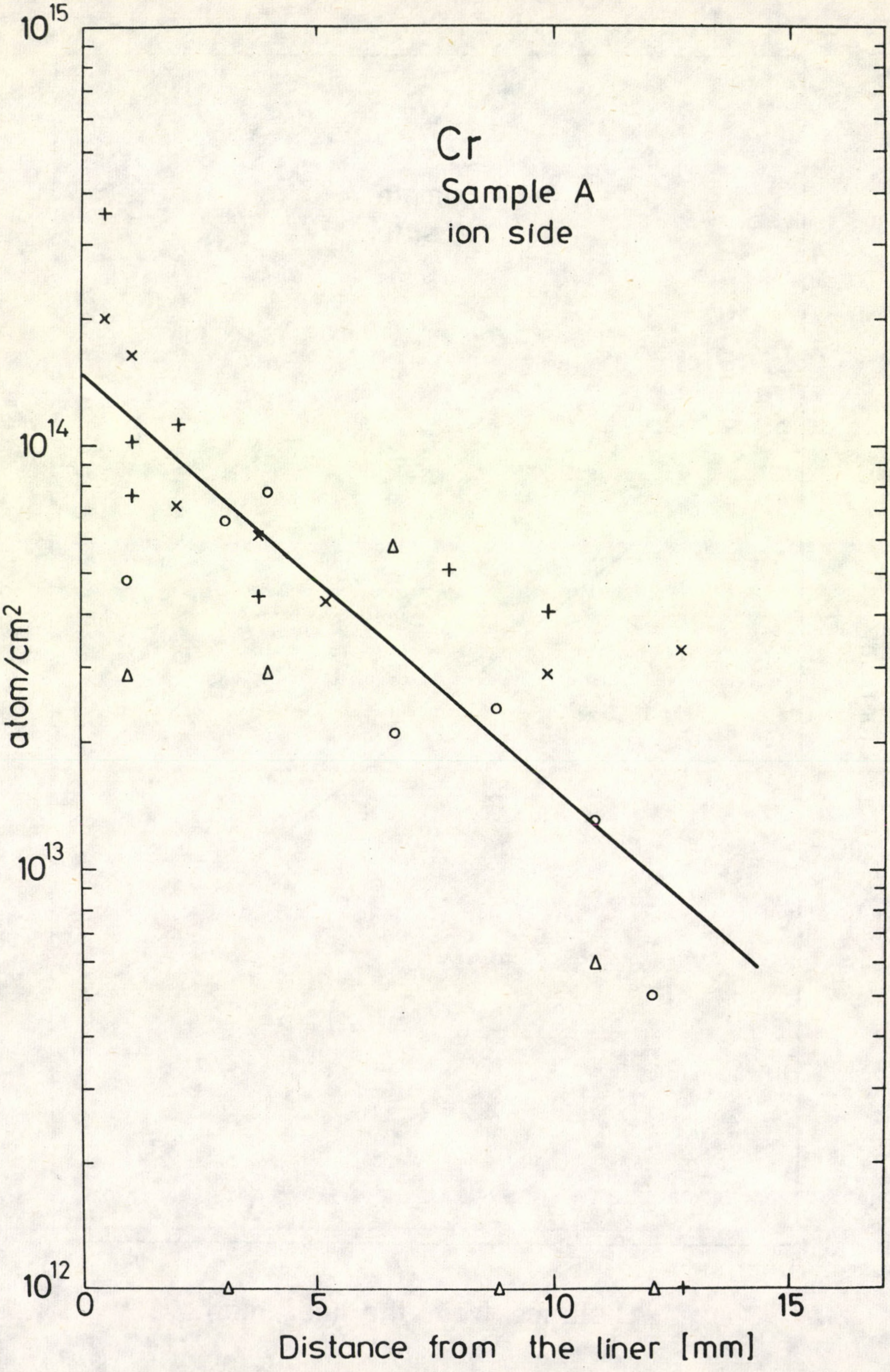
Cr
Sample A
ion side
atom/cm2
10^{15}
10^{14}
10^{13}
10^{12}
0
5
10
15
Distance from the liner [mm]

Fig. 3a

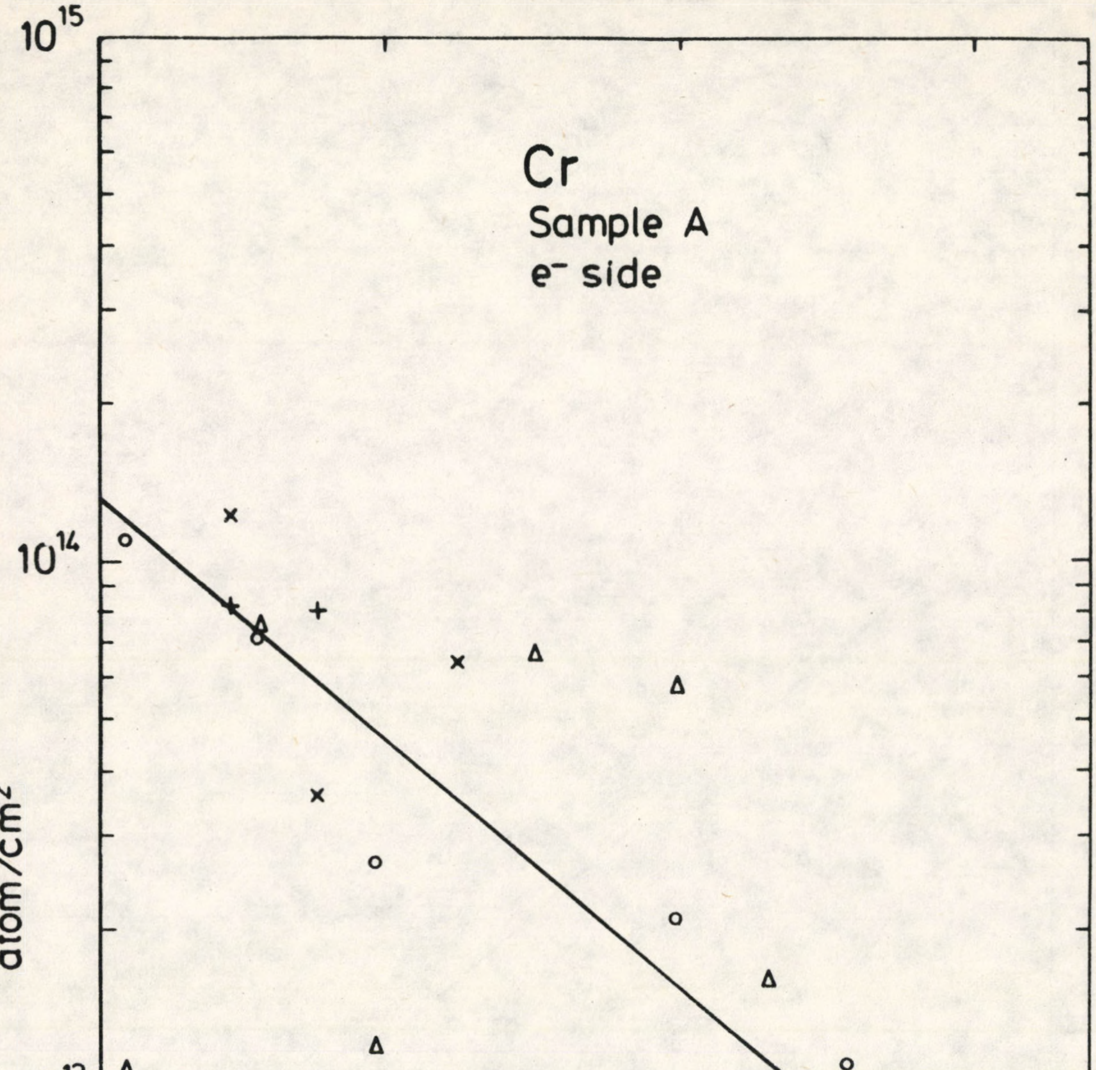
Cr
Sample A
e⁻ side
atom/cm²
10^{15}
10^{14}
10^{13}
10^{12}
0
5
10
15
Distance from the liner [mm]

Fig. 3b

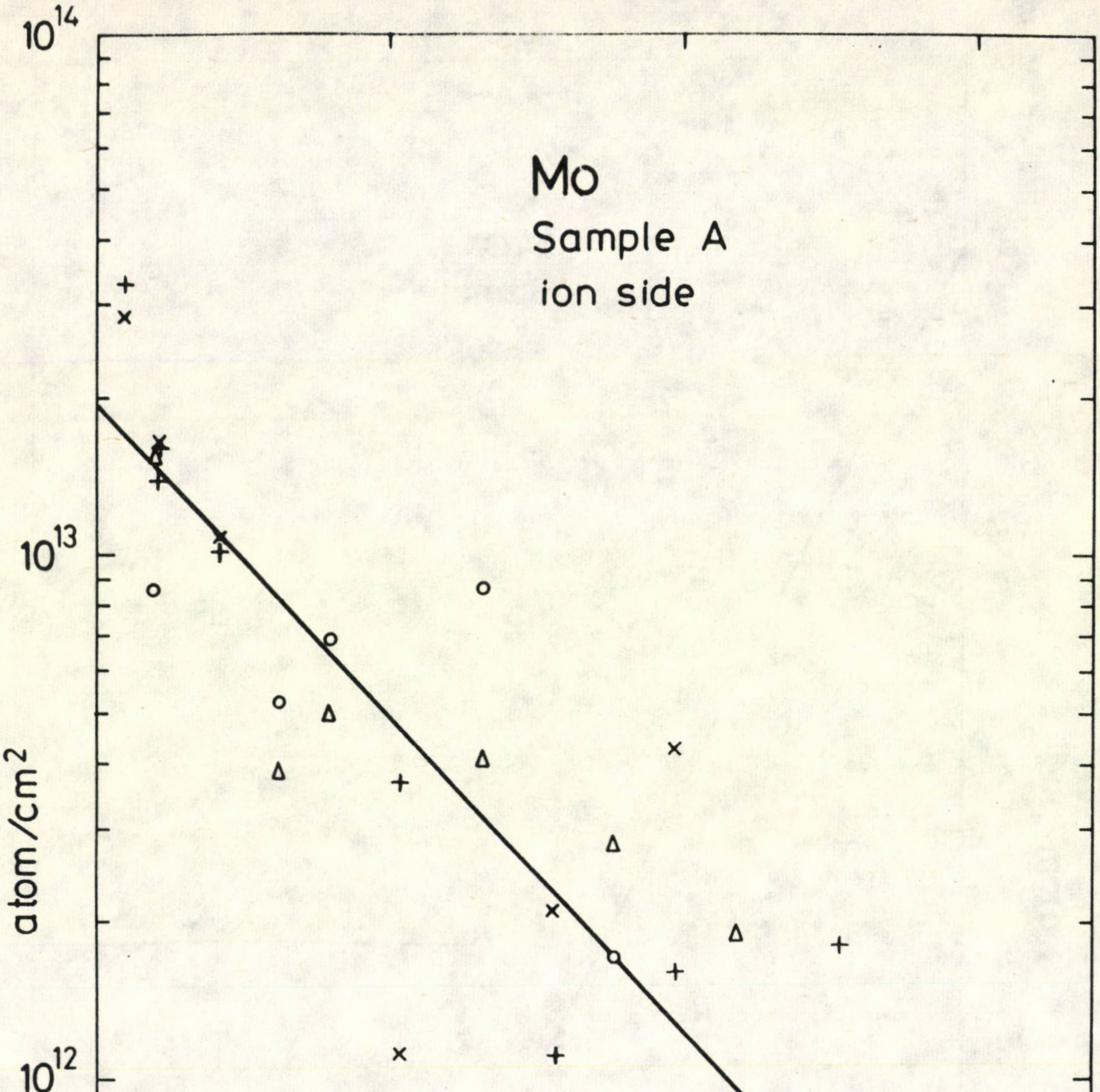
Mo
Sample A
ion side
10^{14}
10^{13}
10^{12}
10^{11}
atom/cm^2
0
5
10
15
Distance from the liner [mm]

Fig.4a

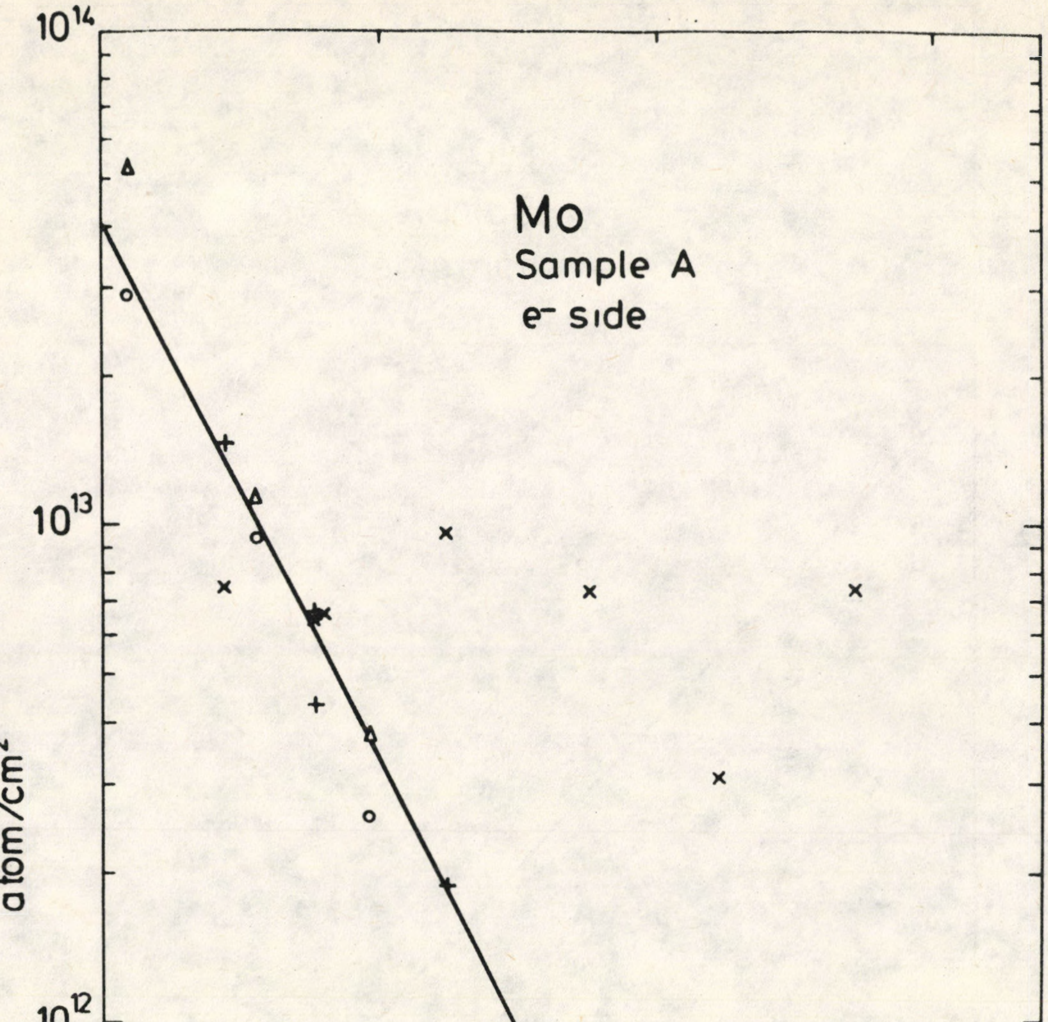

Mo
Sample A
e⁻ side
atom/cm²
10¹⁴
10¹³
10¹²
10¹¹
0
5
10
15
Distance from the liner[mm]

Fig. 4b

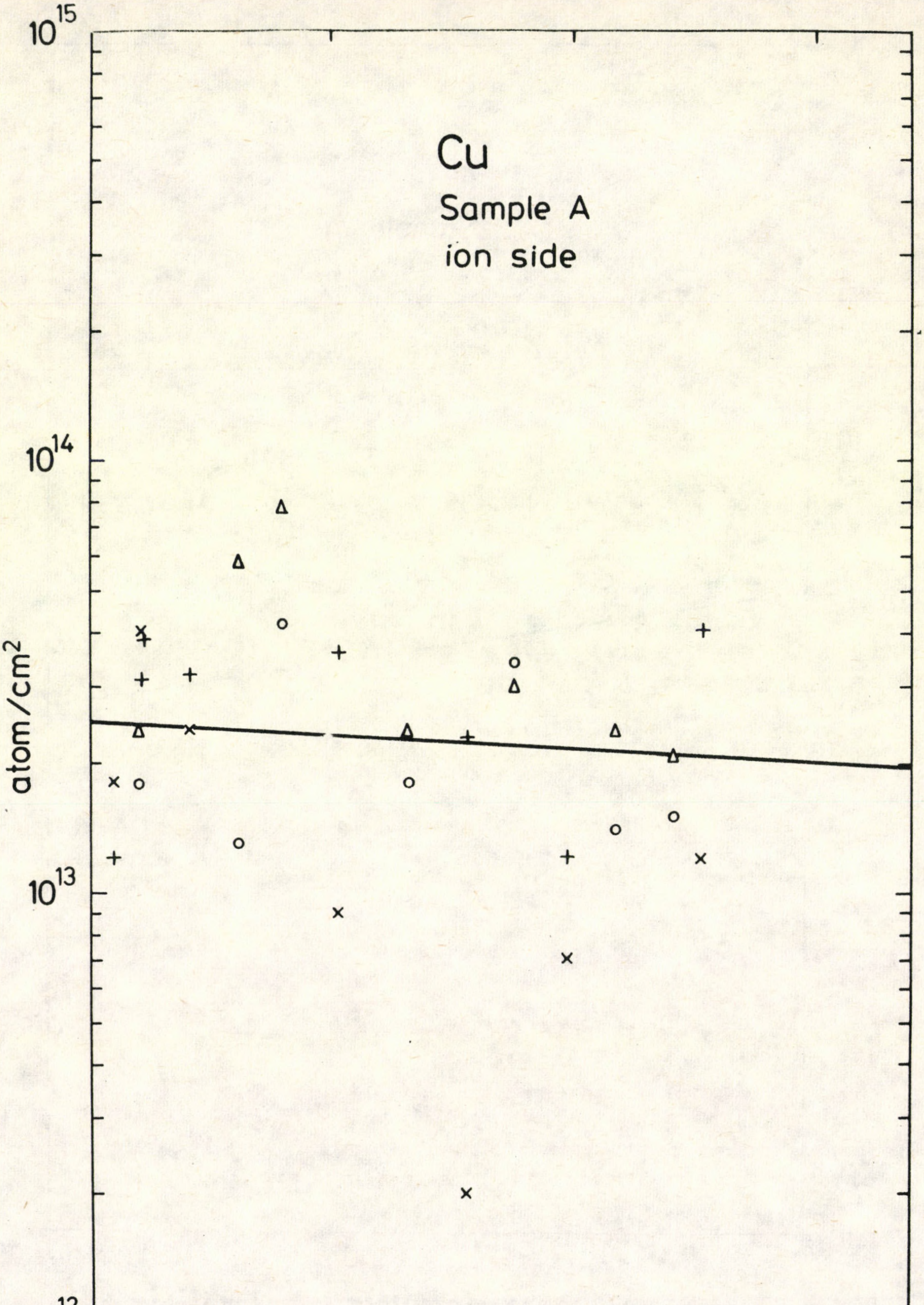
Cu
Sample A
ion side
10^{15}
10^{14}
10^{13}
10^{12}
atom/cm^2
0
5
10
15
Distance from the liner[mm]

Fig. 5a

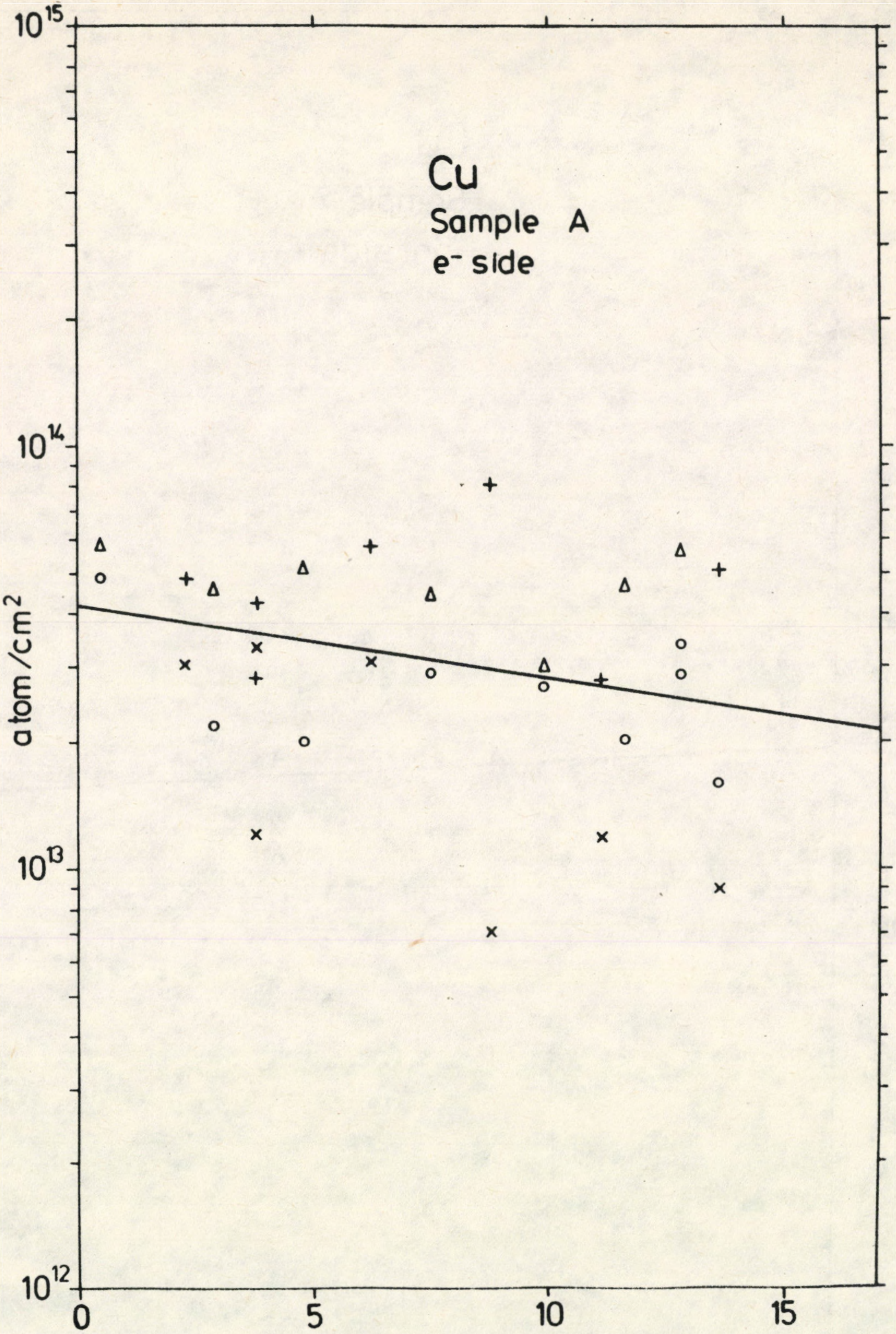
Cu
Sample A
e⁻ side
10^15
10^14
10^13
10^12
atom/cm²
0
5
10
15
Distance from the liner [mm]

Fig.5b

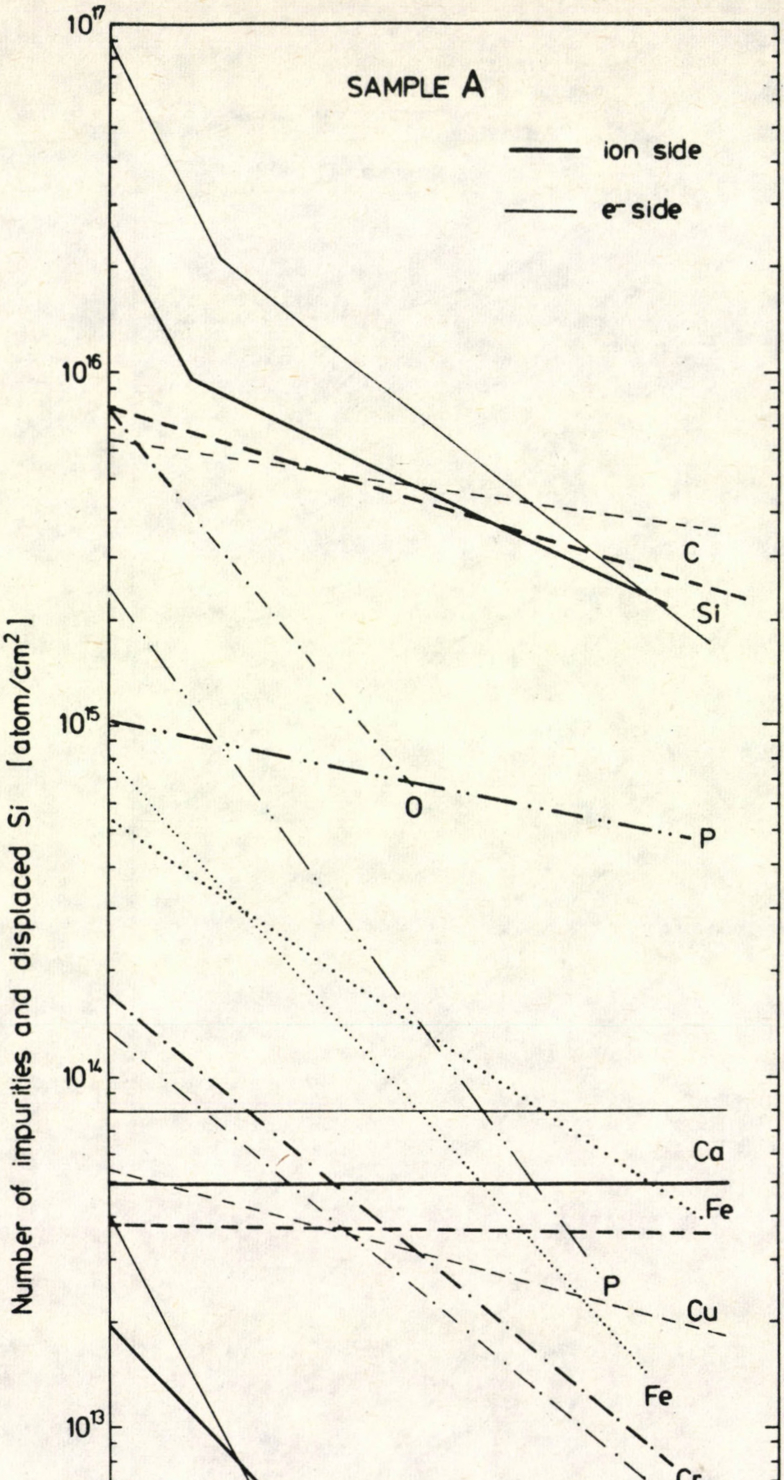
SAMPLE A
ion side
e⁻ side
Number of impurities and displaced Si [atom/cm²]
Distance from the liner [mm]
10¹⁷
10¹⁶
10¹⁵
10¹⁴
10¹³
10¹²
0
5
10
15
C
Si
O
P
Ca
Fe
P
Cu
Fe
Cr
Cd
Mo

Fig. 6.

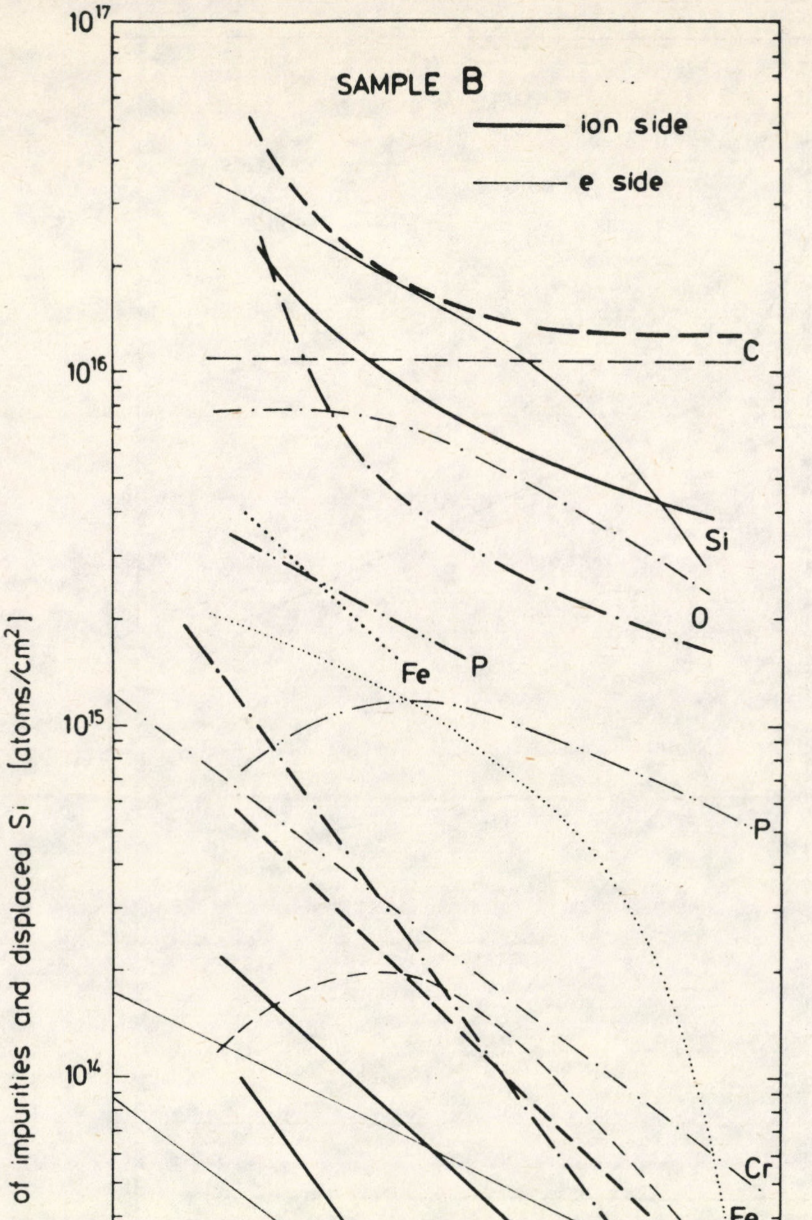

SAMPLE B
ion side
e side
C
Si
Cu
O
P
Fe
P
Cr
Fe
Cu
Ca
Ca
Cr
Mo
Cd
Mo
Cd
10^{17}
10^{16}
10^{15}
10^{14}
10^{13}
10^{12}
Number of impurities and displaced Si [atoms/cm²]
0
5
10
15
Distance from the liner [mm]

Fig. 7.

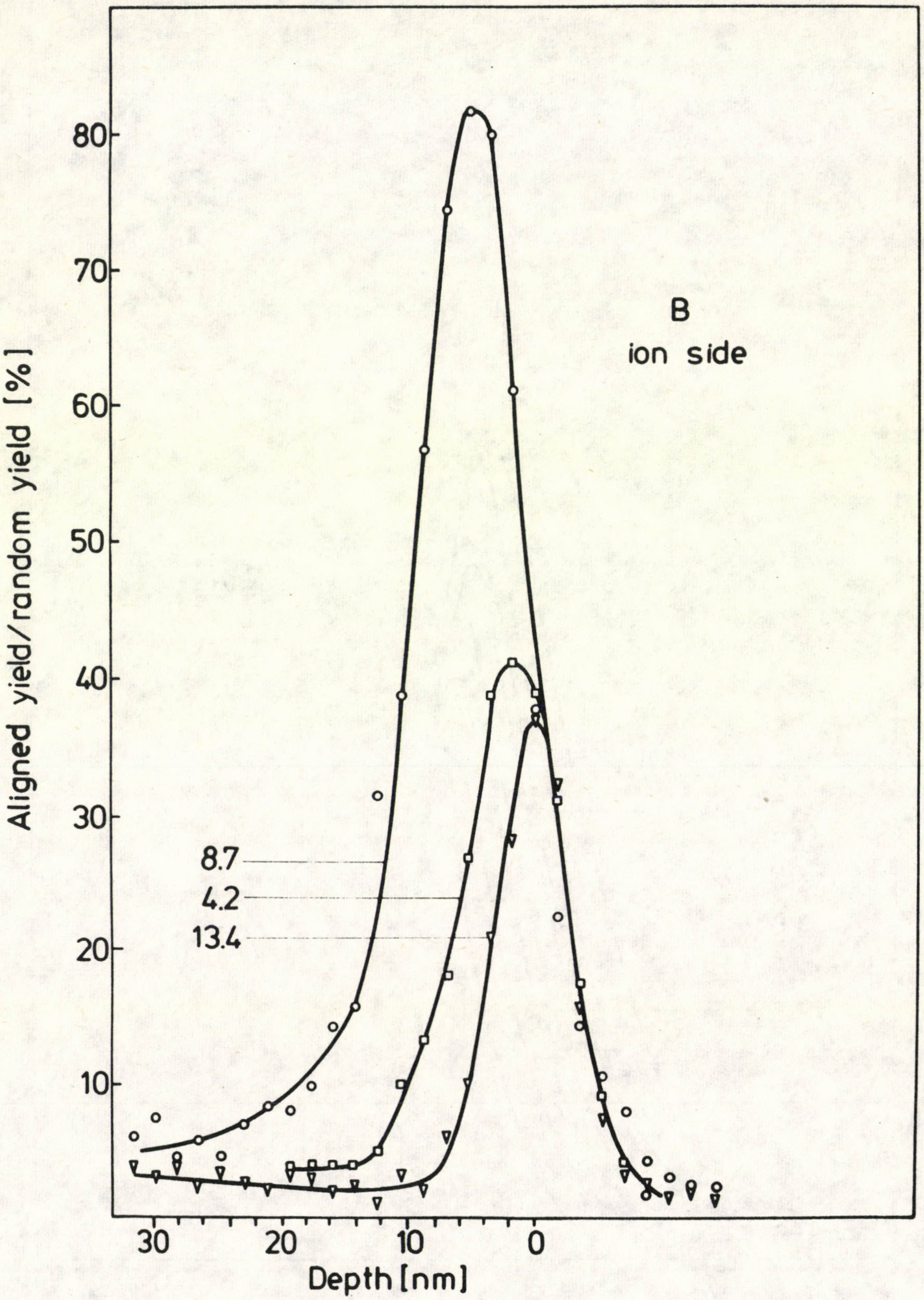
80
70
60
50
40
30
20
10
Aligned yield/random yield [%]
B
ion side
8.7
4.2
13.4
30
20
10
0
Depth [nm]

Fig. 8.

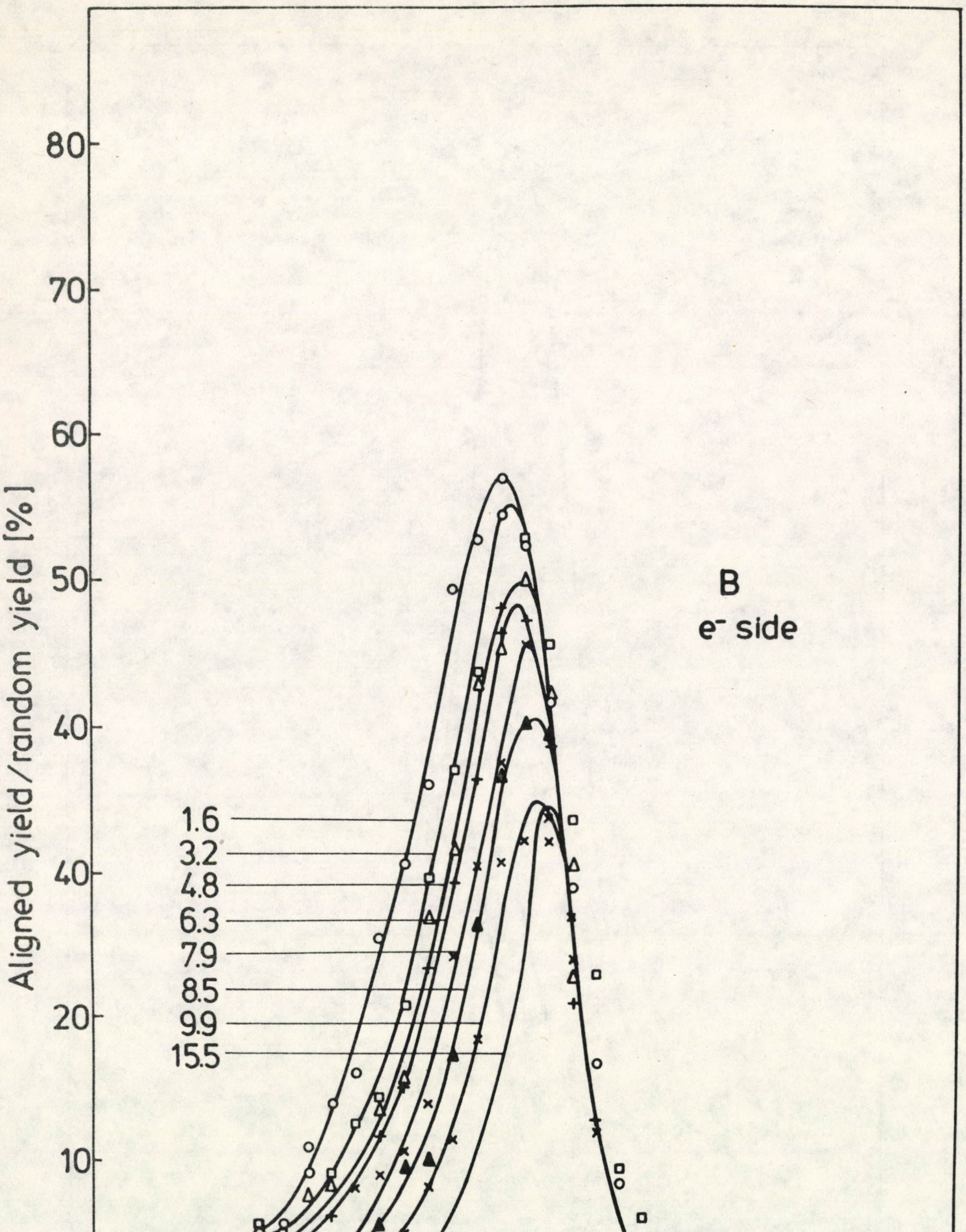
Aligned yield/random yield [%]
80
70
60
50
40
40
20
10
B
e⁻ side
1.6
3.2
4.8
6.3
7.9
8.5
9.9
15.5
30
20
10
0
Depth [nm]

Fig. 9.

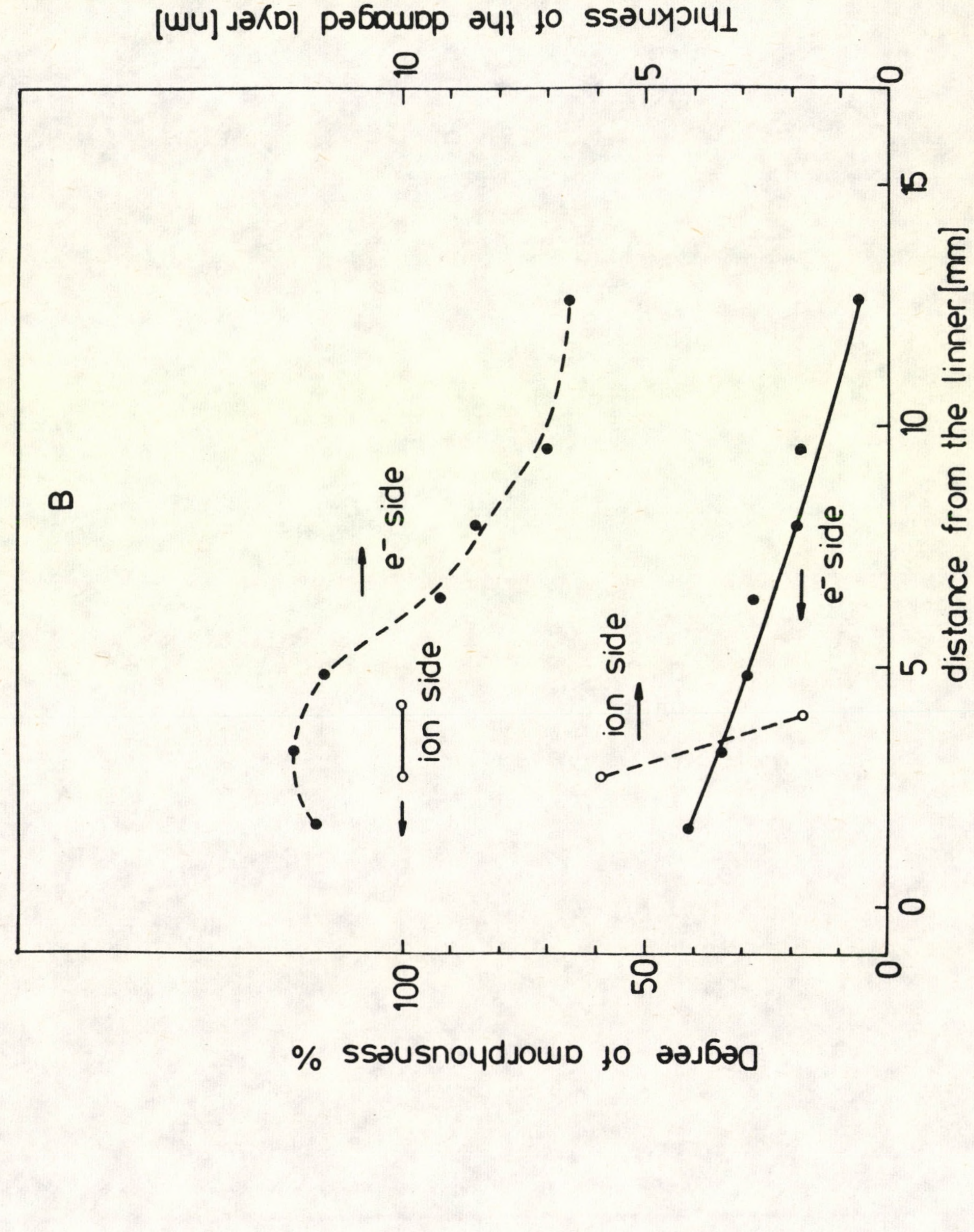
B
ion side
e⁻ side
ion side
e⁻ side
Degree of amorphousness %
0
50
100
Thickness of the damaged layer [nm]
0
5
10
distance from the linner [mm]
0
5
10
15

Fig. 10.

63.140

Kiadja a Központi Fizikai Kutató Intézet
Felelős kiadó: Szegő Károly
Szakmai lektor: Szőkefalvy-Nagy Zoltán
Nyelvi lektor: Pócs Lajos
Példányszám: 605 Törzsszám: 81-236
Készült a KFKI sokszorosító üzemében
Felelős vezető: Nagy Károly
Budapest, 1981. április hó